

Autoclastic subvolcanic rocks in the Tonglu basin, Zhejiang Province, China: a description of “pearlitic border” textures in an adamellite porphyry

ZEN Ja Hu¹⁾ and Kanenori SUWA²⁾

¹⁾Department of Earth Sciences, Nanjing University, Nanjing, China

²⁾Nihon Fukushi University; Professor Emeritus of Nagoya University

(Received August 30, 2002 / Accepted December 25, 2002)

ABSTRACT

Autoclastic rocks are produced in a shallow-level subvolcanic setting by crypto-explosive activity. In many localities around southeastern China, autoclastic subvolcanic rocks were formed between the late Jurassic and the early Cretaceous.

In the Tonglu volcanic basin, three comagmatic stages of volcanic rock have been exposed by deep denudation. First stage rocks consist of rhyolites and rhyodacites and are distributed along the margins of the basin. Third stage hypabyssal intrusions consist of aegirine-riebeckite bearing quartz monzonitic porphyry, and occupy the central basin. Between these stages, autoclastic adamellite porphyry occurs, a subvolcanic rock with porphyritic texture.

Autoclastic adamellite porphyry contains “pearlitic” overgrowths around orthoclase phenocryst. The overgrowths contain quartz intergrown with orthoclase that is optically continuous with the host phenocrysts.

Pearlitic overgrowths also occur around porphyritic plagioclase, quartz and hornblende. Overgrowths around plagioclase contain mostly plagioclase or orthoclase, with lesser quartz. Overgrowths around quartz phenocrysts are predominantly quartz, with lesser amounts of orthoclase. Overgrowths around hornblende phenocrysts are mostly composed of hornblende with lesser quartz and orthoclase.

In general, the pearlitic overgrowths have compositions that are intermediate between the phenocrysts and the groundmass. The overgrowths may therefore represent reaction textures that developed in an autoclastic environment.

1. Introduction

Autoclastic rocks are produced in a shallow-level subvolcanic setting by crypto-explosive activity. In southeastern China, the distribution of autoclastic subvolcanic rocks is generally controlled by northeast-trending regional faults. These lithologies are formed in late Jurassic to early Cretaceous Periods.

The Tonglu area of Zhejiang Province is situated at 119.6° E and 29.8° N, about 65 km southwest of Hangzhou. Autoclastic subvolcanic rocks occur in the fault-bounded Tonglu basin, as a narrow northeast-trending zone (Fig. 1). Three comagmatic stages of volcanic rocks have been exposed by deep denudation. The first stage consists of rhyolites and rhyodacites that are distributed along the margins of the basin. Third stage hypabyssal intrusions consist of aegirine-riebeckite bearing quartz monzonitic porphyry, and occupy the central basin. Between these stages, autoclastic adamellite

porphyry occurs, a subvolcanic rock with porphyritic texture. In several locations, autoclastic subvolcanic rocks intrude into Ordovician to Permian sedimentary lithologies, including sandstone, mudstone, shale, conglomerate and limestone.

Petrological studies of the Tonglu autoclastic subvolcanic rocks revealed the presence of overgrowth textures around orthoclase phenocrysts, which were described as "pearlitic borders" (Wang and Zhou, 1986).

Pearlitic borders also occur around porphyritic plagioclase, quartz and hornblende. In this paper, these pearlitic borders are described in detail. Chemical compositions of minerals in the pearlitic borders and in the third stage aegirine-riebeckite bearing quartz monzonitic porphyry are also discussed.

2. Distribution of the autoclastic adamellite porphyry

A geological sketch map of the Tonglu volcanic basin, based on Wang and Zhou (1986), is shown in Fig. 1. The distributions of the three volcanic stages and the sample

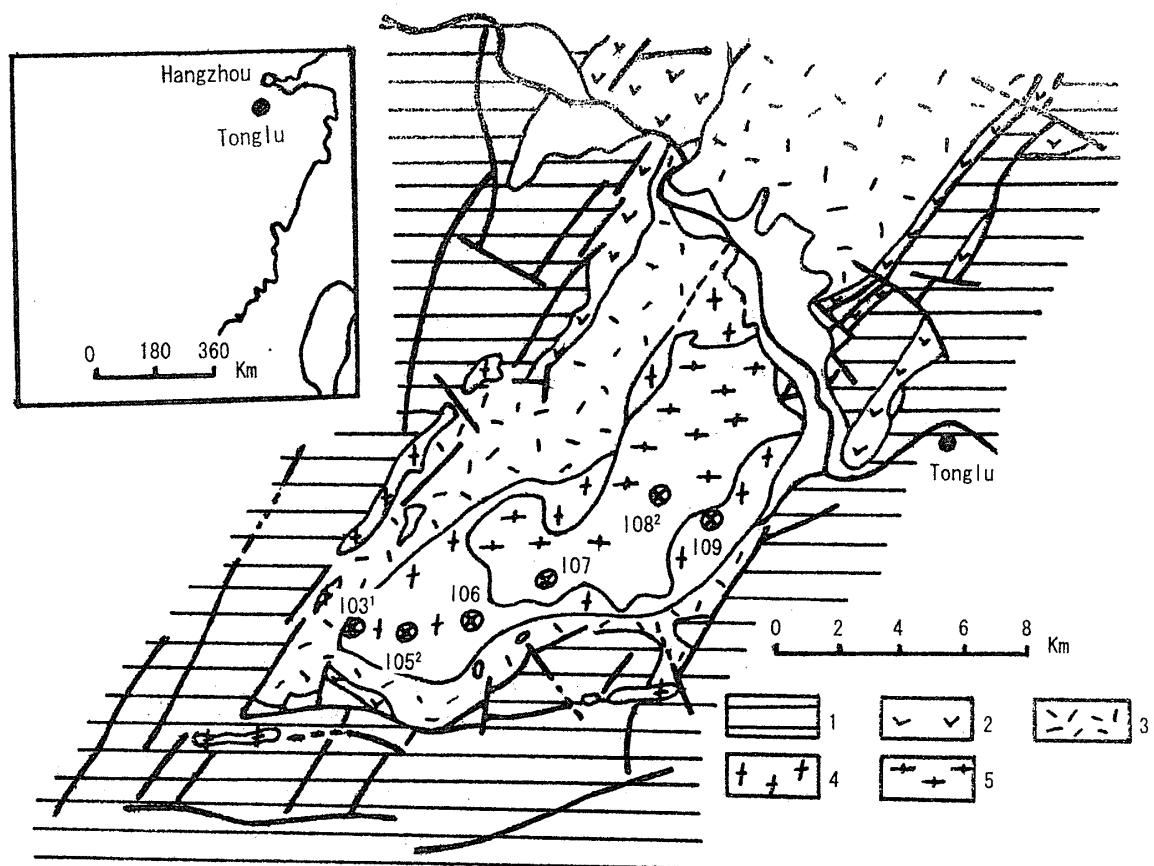


Fig. 1. Geologic sketch map of Tonglu volcanic basin (Wang · Zhou, 1986) and Locality points of rock sampling.

1. Pre-Jurassic strata
2. Laocun formation (early Jurassic volcanic and sedimentary rocks) (J_3l)
3. Huangjian formation (middle Jurassic volcanic rock) (J_3h) (1st stage)
4. autoclastic adamellite porphyry (J_3c) (2nd stage)
5. quartz monzonitic porphyry ($\delta o (t)$) (3rd stage)

locations are shown. For the second stage autoclastic adamellite porphyry, Wang and Zhou (1986) measured 2V values for porphyritic potash feldspar crystals with low triclinicity 0.2–0.3 along each profile and plotted two isopleths (40° and 50°) of optical angle on a geological sketch map (Fig. 2). The shape of the 2V isopleths is similar to the outline of boundary between the second stage autoclastic adamellite porphyry and the first stage rhyolitic and rhyodacitic volcanic rocks. The 2V=40° isopleth lies near the boundary against the first stage volcanic rocks, while the 2V=50° isopleth is more distant. It was suggested by Wang and Zhou (1986) that the 2V=40° isopleth indicates a higher temperature of crystallisation closer to the volcanic stage boundary.

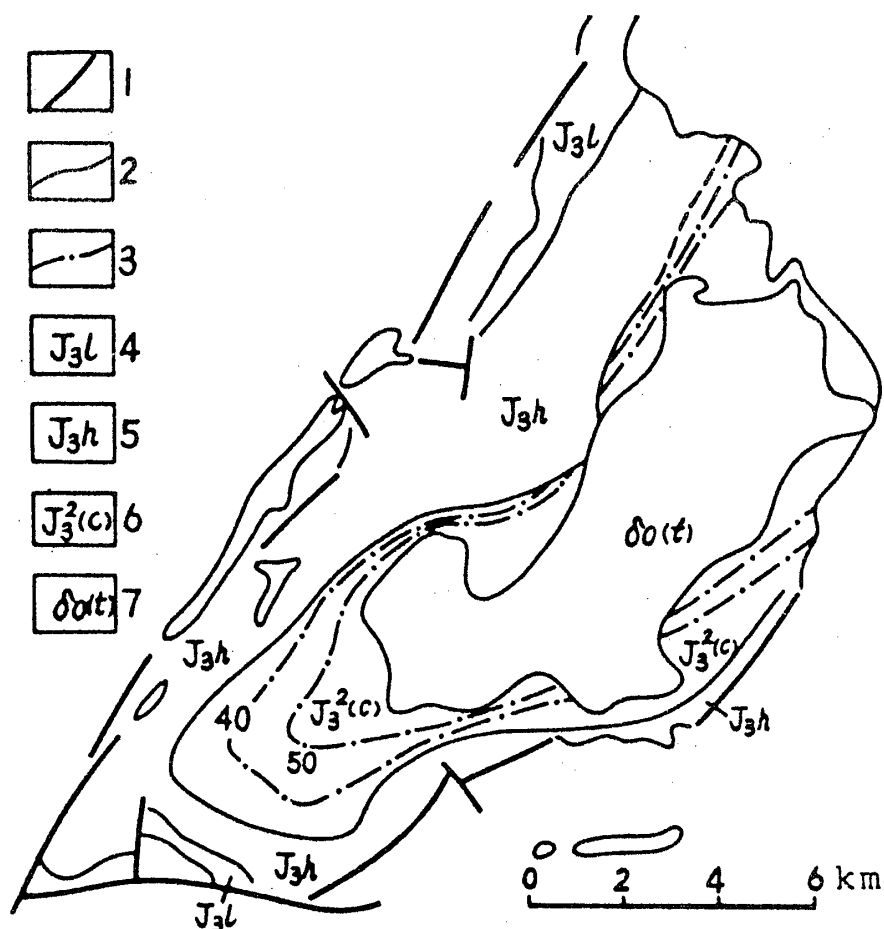


Fig. 2. The isopleth of optical angle of orthoclase in autoclastic adamellite porphyry (Wang · Zhou, 1986)

1. fault
2. geologic boundary
3. isopleth of optical angle
4. Laocun formation (J_3l)
5. Huangjian formation (J_3h) (1st stage)
6. autoclastic adamellite porphyry ($J_3^2(c)$) (2nd stage)
7. quartz monzonitic porphyry ($\delta o(t)$) (3rd stage)

3. Petrography of autoclastic adamellite porphyry

The autoclastic adamellite porphyry of the second volcanic stage is mainly composed of orthoclase, plagioclase, quartz, biotite, and hornblende, with accessory amounts of zircon, apatite, magnetite, sphene, and allanite. Chlorite, epidote, sericite, and kaolinite occur as secondary minerals. An average chemical composition of eight specimens of autoclastic adamellite porphyry is shown in Table 1 (Wang and Zhou, 1986).

In this study, four specimens of autoclastic adamellite porphyry were examined. Specimens I03¹ and I05² were found near the boundary with the first stage volcanic rocks, and specimens I06 and I09 were more distant (Fig. 1). Based on the 2V studies by Wang and Zhou (1986), specimens I03¹ and I05² are considered to have formed at higher temperatures than specimens I06 and I09. Mineral modes for the samples are shown in Table 2. Generally, phenocrysts occupy about 60% by volume.

Table 1. Chemical composition of autoclastic adamellite porphyry (Wang · Zhou, 1986)

SiO ₂	TiO ₂	Al ₂ O ₃	Fe ₂ O ₃	FeO	MnO	MgO	CaO	Na ₂ O	K ₂ O	P ₂ O ₅	H ₂ O(+)	Total
67.99	0.46	14.74	0.88	2.68	0.08	0.93	2.31	3.56	4.32	0.15	1.92	100.02

Table 2. Mode of minerals of autoclastic adamellite porphyry

Phenocryst	I03 ¹	I05 ²	I06	I09
Orthoclase	25%	27%	30%	15%
Plagioclase	43	36	34	45
Quartz	22	26	10	16
Biotite	6	7	14	15
Hornblende	3	4	12	9

Groundmass	I03 ¹	I05 ²	I06	I09
Orthoclase	50%	52%	47%	48%
Plagioclase	7	8	17	12
Quartz	38	34	30	32
Biotite	4	6	4	6
Hornblende	—	—	2	2

Whole rock	I03 ¹	I05 ²	I06	I09
Orthoclase	35%	37%	36.8%	28.9%
Plagioclase	28.6	24.8	27.2	31.1
Quartz	28.4	29.2	18	22.7
Biotite	5.2	6.6	10	11.2
Hornblende	1.8	2.4	8	6.2
Total	99.0	100.0	100.0	100.1

4. Pearlitic borders around orthoclase phenocryst

Pearlitic overgrowth borders are common around orthoclase phenocrysts (Photos 1–5). The pearlitic textures are mainly composed of orthoclase, with inclusions of

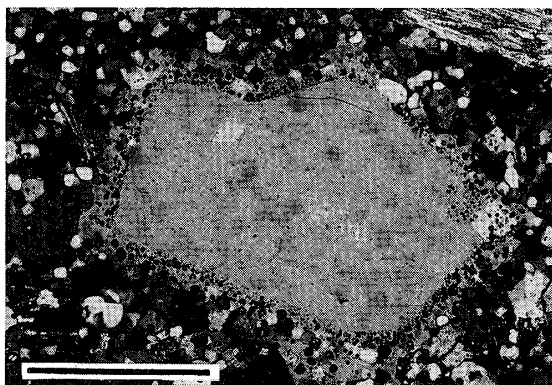


Photo 1. Orthoclase phenocryst and its “pearlitic border” in autoclastic adamellite porphyry I03¹. Nicols crossed. Length of bar: 0.2mm.

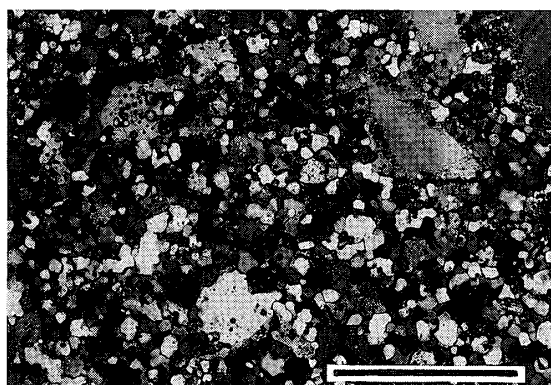


Photo 2. Autoclastic adamellite porphyry I03¹. Note the formation of embryonic “pearlitic border” around fine-grained orthoclase crystal (~0.05~0.1mm). Nicols crossed. Length of bar: 0.2mm.

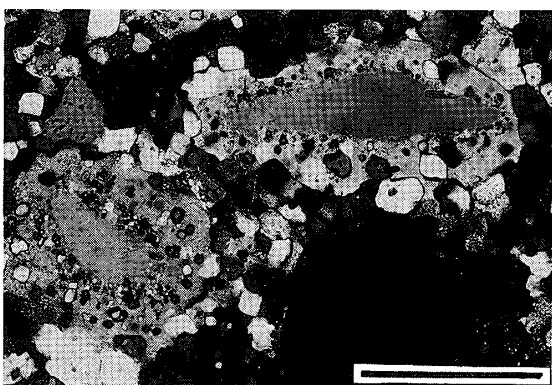


Photo 3. Orthoclase phenocryst and its “pearlitic border” in autoclastic adamellite porphyry I05². Nicols crossed. Length of bar: 0.2mm.

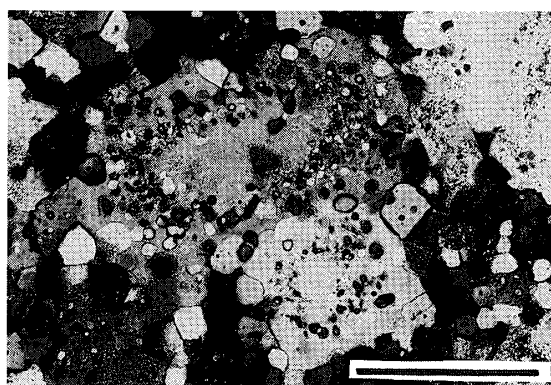


Photo 4. Orthoclase phenocryst and its “pearlitic border” in autoclastic adamellite porphyry I06. Nicols crossed. Length of bar: 0.2mm.

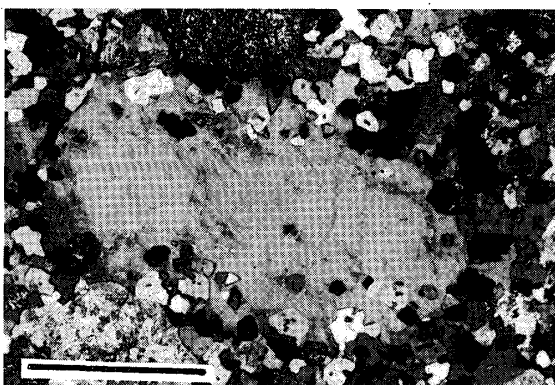


Photo 5. Orthoclase phenocryst and its “pearlitic border” in autoclastic adamellite porphyry I09. Nicols crossed. Minerals constituting “pearlitic border” have increased in grain size, and “pearlitic border” becomes ambiguous. Length of bar: 0.5mm.

quartz, magnetite, biotite, apatite, and zircon. The optical orientation of orthoclase in a pearly border is continuous with that of host orthoclase, but the optical orientation of poikilitic quartz grains are variable. Pearly borders vary in width from 0.03 mm to 0.02 mm. The pearly borders are narrower in I03¹ (0.03–0.045 mm) than in specimen I09 (0.12–0.18 mm), which is considered to have formed under lower temperatures. Inside every pearly border, quartz grains close to host orthoclase phenocryst are small and coarsen gradually as they approach the surrounding groundmass. Quartz grains are finer in the narrower pearly borders in specimen I03¹ than in specimen I09. These relationships are summarized in Table 3.

Table 3. Pearly border around orthoclase phenocryst

	Width of pearly border	Grain size of quartz in pearly border
I03 ¹	0.03 – 0.045mm	0.002 – 0.016 mm
I05 ²	0.056 – 0.12 mm	0.004 – 0.03 mm
I 0 6	0.064 – 0.14 mm	0.006 – 0.04 mm
I 0 9	0.12 – 0.18 mm	0.02 – 0.13 mm

Table 4. Grain size of orthoclase, plagioclase and quartz in groundmass

	Orthoclase	Plagioclase	Quartz
I03 ¹	0.016–0.024mm	about 0.044mm	about 0.02mm
I05 ²	0.024–0.056mm	about 0.088mm	about 0.04mm
I 0 6	0.032–0.08 mm	about 0.092mm	about 0.048mm
I 0 9	0.028–0.12 mm	about 0.14mm	about 0.064mm

Table 5. Chemical compositions of orthoclase phenocryst, orthoclase in pearly border, and orthoclase in groundmass

	Phenocryst	Pearly border	Groundmass
I03 ¹	Or70.0–Or72.6	Or71.6–Or94.6	Or72.2–Or82.4
	Ab30.0–Ab27.4	Ab28.4–Ab5.4	Ab27.8–Ab17.6
	An0.0–An0.0	An 0.0–An 0.0	An 0.0–An 0.0
I05 ²	Or64.1–Or81.6	Or63.8–Or71.4	Or65.8–Or71.9
	Ab33.4–Ab18.4	Ab35.2–Ab28.6	Ab32.7–Ab28.1
	An 2.5–An 0.0	An 1.0–An 0.0	An 1.5–An 0.0
I 0 6	Or64.4–Or73.1	Or72.0–Or87.5	Or74.6–Or88.9
	Ab34.0–Ab25.7	Ab27.3–Ab12.2	Ab24.8–Ab11.1
	An 1.6–An 1.2	An 0.7–An 0.3	An 0.6–An 0.0
I 0 9	Or65.5–Or86.0	Or65.5–Or94.5	Or67.0–Or94.5
	Ab33.2–Ab13.6	Ab30.7–Ab 5.1	Ab32.4–Ab 5.5
	An 1.3–An 0.4	An 3.8–An 0.4	An 0.6–An 0.0

Orthoclase is the main groundmass constituent in autoclastic adamellite porphyry (Table 2). Groundmass orthoclase grains are finer in specimen I03¹ than in specimen I09 (Table 4). Embryonic pearlitic borders occur around fine-grained orthoclase crystals (Photo 2). Pearlitic borders are difficult to distinguish from the groundmass where the latter is relatively coarse (Photo 5).

Chemical compositions of orthoclase in phenocrysts, pearlitic borders, and the groundmass are shown in Table 5. Orthoclase is less potassic in phenocrysts than in pearlitic borders, and orthoclase in groundmass is the most potassic. All orthoclase analyses have very low An contents (Table 5).

5. Pearlitic borders around plagioclase phenocryst

Pearlitic borders around plagioclase phenocryst vary from well to partially developed, and are absent in some cases. They are mostly composed of plagioclase or orthoclase, with intergrown quartz grains. In specimen I03¹, around 60% of plagioclase phenocrysts have pearlitic borders, which are narrow (0.014–0.03 mm) and typically incomplete. In contrast, pearlitic borders in specimen I05² are well developed and wider (0.025–0.064 mm). Pearlitic borders around plagioclase phenocryst are well developed in specimen I06, with widths of 0.03–0.10 mm. The borders are absent from porphyritic plagioclase in specimen I09. Within the pearlitic borders, quartz grains coarsen from plagioclase phenocryst to groundmass. Generally, quartz grains are finer in plagioclase borders from specimen I03¹ than from specimen I06. These relationships are summarized in Table 6.

Plagioclase in each pearlitic border is optically continuous with that in the host phenocryst, whereas the optical orientation of poikilitic quartz is variable. Plagioclase is a minor component of the groundmass (7–17%; Table 2). Plagioclase grains in the groundmass are finer and subhedral in specimen I03¹, and coarser and are subhedral to euhedral in specimen I09 (Table 4). Plagioclase phenocrysts are commonly zoned in specimens I03¹, I05², and I09. Specimen I06 contains zoned and unzoned

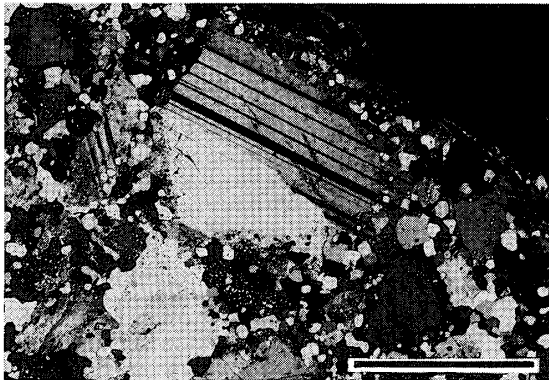


Photo 6. Plagioclase phenocryst and its "pearlitic border" in autoclastic adamellite porphyry I05². Nicols crossed. Length of bar: 0.5mm.

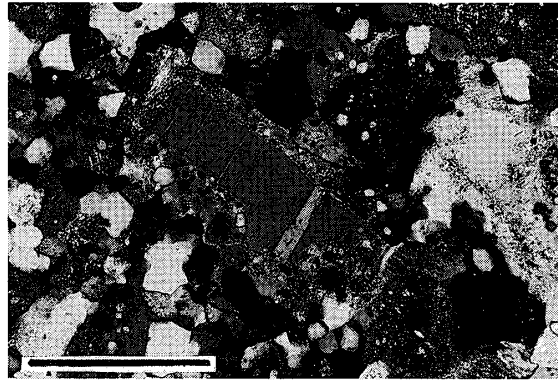


Photo 7. Plagioclase phenocryst and its "pearlitic border" in autoclastic adamellite porphyry I06. Nicols crossed. Length of bar: 0.2mm.

Table 6. Pearlitic border around plagioclase phenocryst

	Width of pearlitic border	Grain size of quartz in pearlitic border	Developing pattern of pearlitic border	Developing frequency of pearlitic border
I03 ¹	0.014–0.03 mm	0.004–0.016mm	partially	60%
I05 ²	0.025–0.064 mm	0.005–0.02 mm	mostly	60–70%
I06	0.03–0.10 mm	0.006–0.026mm	well-developed	100%
I09	—	—	—	0%

Table 7. Chemical compositions of plagioclase phenocryst, plagioclase or orthoclase in pearlitic border, and plagioclase in groundmass

	Phenocryst	Pearlitic border	Groundmass
I03 ¹	Ab42.5–Ab73.3 An55.9–An22.0 Or 1.6–Or 4.7		Ab61.7–Ab81.1 An36.9–An15.1 Or 1.4–Or 3.8
I05 ²	Ab58.0–Ab67.6 An39.5–An27.2 Or 2.5–Or 5.2	Ab72.1–Ab77.7 An24.2–An15.7 Or 3.7–Or 6.6	Ab65.0–Ab70.2 An31.2–An22.3 Or 3.8–Or 7.5
I06	Ab64.9–Ab67.8 An30.7–An27.3 Or 4.4–Or 4.9	Or71.7–Or68.1 Ab27.8–Ab31.5 An 0.5–An 0.4	Ab64.6–Ab67.0 An31.7–An28.2 Or 3.7–Or 4.8
I09	Ab54.5–Ab73.2 An43.0–An22.0 Or 2.5–Or 4.8	/	Ab68.4–Ab73.8 An29.2–An22.1 Or 2.4–Or 4.1

plagioclase phenocryst.

Chemical compositions of plagioclase in phenocrysts, pearlitic borders, and the groundmass are shown in Table 7. Plagioclase is less sodic in phenocrysts than in pearlitic borders, and plagioclase in groundmass is the most sodic.

6. Pearlitic borders around quartz phenocryst

Pearlitic borders around quartz phenocryst have similar features to those around feldspars. They contain quartz and lesser orthoclase, which coarsens away from the host quartz grain. Pearlitic magnetite grains are sometimes also present. Pearlitic borders around quartz are absent in the I03¹ and only partially developed in specimen I05², where they are narrow (0.04–0.072 mm), and fine-grained (0.007–0.028 mm). Pearlitic borders around quartz phenocryst are only partially developed in specimen I06, but are wider than those in specimen I05². In specimen I09, the borders around quartz are well-developed (0.06–0.128 mm) and show outward coarsening in orthoclase grains (0.008 to 0.064 mm).

Quartz phenocryst commonly has undulatory extinction and corroded margins (Photo 8). Quartz grains in the groundmass are subhedral or anhedral. Groundmass quartz is finer in specimen I03¹ (0.02mm) than in specimen I09 (0.064 mm, Table 4).

7. Pearlitic borders around hornblende phenocryst

Pearlitic borders around hornblende phenocryst (Photos 9–11) are mostly composed of hornblende, with lesser orthoclase, plagioclase and quartz. Grains in the pearlitic border become coarser away from the host grain. The optical orientation of hornblende in a pearlitic border is continuous with that of host hornblende. Biotite occurs in some pearlitic borders in specimen I03¹. Hornblende is widely altered to chlorite and epidote in specimen I05², where pearlitic borders are vague. The horn-

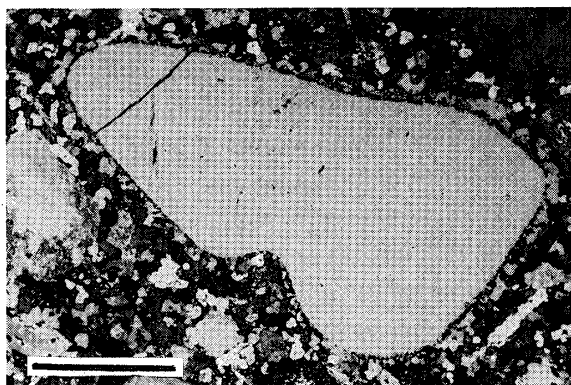


Photo 8. Quartz phenocryst and its "pearlitic border" in autoclastic adamellite porphyry I09. Nicols crossed. Length of bar: 1mm.

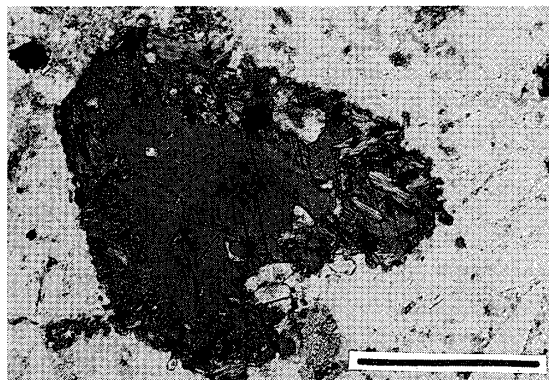


Photo 9. Hornblende phenocryst and its "pearlitic border" in autoclastic adamellite porphyry I03¹. One nicol. Length of bar: 0.5mm.

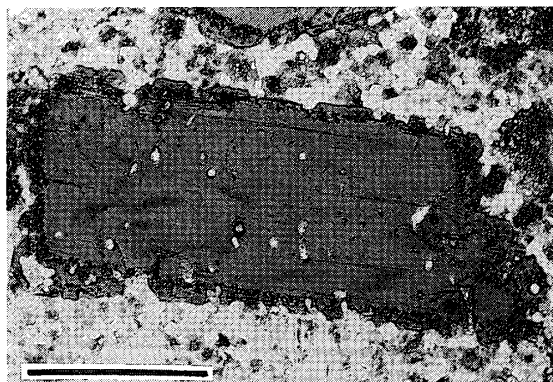


Photo 10. Hornblende phenocryst and its "pearlitic border" in autoclastic adamellite porphyry I06. One nicol. Length of bar: 0.5mm.

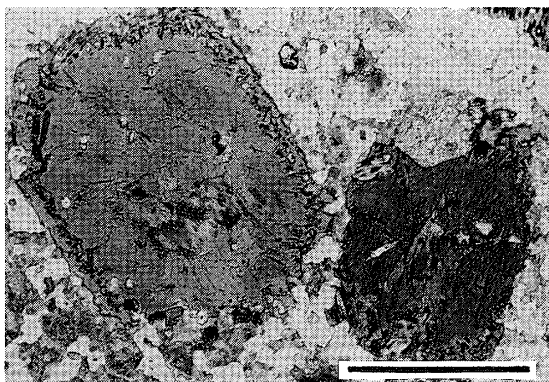


Photo 11. Hornblende phenocryst and its "pearlitic border" in autoclastic adamellite porphyry I09. One nicol. Length of bar: 0.5mm.

blende phenocryst in specimen I03¹ is ferroedenite, and plots near the edenite field. The hornblende phenocrysts in specimens I05² and I06 are ferroedenitic hornblende, and plot near the edenitic hornblende field. Hornblende Al^{IV} are lower in specimen I03¹ than in specimen I05². Orthoclase grains in peralitic borders around hornblende in specimen I06 are Or93.3–Or70.4 (average Or80.1), Ab28.9–Ab6.4 (average Ab19.3), and An0.7–An0.3 (average An0.6). Orthoclase in the groundmass has a similar composition. Plagioclase in peralitic borders from specimen I06 are Ab75.7–Ab73.9 (average Ab74.8), An22.7–An22.5 (average An22.6), and Or3.6–Or1.6 (average Or2.6). This chemical composition of plagioclase grains in peralitic border in the specimen I06 is higher than in Ab molecule than that of groundmass plagioclase, which has a lower Ab content (average Ab66.0 An29.6 Or4.4).

Hornblende phenocryst in specimen I09 is ferroan pargasitic, and peralitic hornblende is of ferroedenite near edenite field. Hornblende phenocrysts have Al^{IV} in the range 1.69–1.60 (average Al^{IV}=1.66), Ti=0.38, and Na+K=0.83–0.78 (average Na+K=0.80). Ferroedenite in the peralitic borders has Al^{IV} values of 1.02–0.94 (average Al^{IV}=0.97), Ti=0.14, and Na+K=0.58–0.56 (average Na+K=0.57). Higher values of Al^{IV}, Ti, and Na+K in hornblende phenocryst than in the peralitic borders indicate that the peralitic borders formed at lower temperatures.

8. Petrogenesis of the peralitic borders

Overgrowths around orthoclase phenocryst were first described by Wang and Zhou (1986), who called them "peralitic borders". These textures are only found in the autoclastic adamellite porphyry, which is the second stage subvolcanic rock in the Tonglu volcanic basin. Wang and Zhou (1986) suggested that the textures are a product of supercooling in the host magma. When magma is rapidly transported from a magma chamber to a shallow-level or surficial setting, pre-existing phenocrysts became cooler than the surrounding magma. Under these conditions, the nucleation density of quartz is nine times greater than that of orthoclase. The growth rate of orthoclase, however, is much higher of that of quartz. Rapid growth of new orthoclase occurred on the margins of pre-existing phenocrysts, as continuous overgrowths. These overgrowths entrained numerous small grains of quartz, forming a peralitic texture. Since the degree of supercooling is highest adjacent to the phenocrysts, entrainment is more rapid and the quartz grains are smaller. Subsequent growth produces overgrowths with quartz inclusions that become gradually larger as the overgrowth increases in width (Wang and Zhou, 1986). Small peralitic borders can even form on small pre-existing orthoclase crystals, as in specimen I03¹ (Photo 2).

In this study, peralitic borders have also been described around porphyritic grains of plagioclase, quartz, and hornblende. The chemical compositions of peralitic border minerals are intermediate between the porphyritic minerals and those in the groundmass. Where the groundmass is coarse-grained and therefore slowly crystallised, such as in specimen I09, peralitic borders are poorly developed or absent. The values of Al^{IV}, Ti and Na+K in hornblende phenocryst are higher than in peralitic border hornblende, indicating that the latter formed under lower temperatures.

9. Petrography and chemistry of the quartz monzonitic porphyry

Specimen I07 is composed of plagioclase (38%), potash feldspar (33%), quartz (16%), biotite (7%), hornblende (3%), and orthopyroxene (1%), with accessory amounts of magnetite (1%), apatite (0.5%), and zircon (0.1%). Chlorite, epidote, and sericite occur as secondary minerals. The sample has a monzonitic texture (Photo 12), with fine-grained plagioclase and quartz crystals entrained within coarse-grained potash feldspar. Plagioclase mostly occurs as platy euhedral crystals with albite, pericline and albite-Carlsbad law twinning. Normal and oscillatory zoning is common. One grain has a zoning sequence as follows: An 48 (core) → An 35 → An 52 → An 49 → An 42 → An 31 → An 29 → An 26 (rim). Or content is in the range Or3.1–Or1.4 (average Or 2.3). Potash feldspar grains are of 0.2 mm–2.4 mm across and exhibit perthitic structures. Or content is in the range Or75.3–Or59.1 (average Or 67.4), Ab39.7–Ab24.3 (average Ab31.9), An1.2–An0.4 (average An0.8). Quartz occurs as anhedral crystals 0.18 mm–1.4 mm across and along feldspar grain boundaries. Quartz typically has undulatory extinction. Biotite is present as 0.1 mm–1.2 mm long flakes. Mg/(Mg+Fe+Mn+Al^{IV}+Ti) in biotite is 0.40, and (Al^{IV}+Ti)/(Mg+Fe+Mn+Al^{IV}+Ti) is 0.09. Hornblende occurs as subhedral or euhedral tabular crystals 0.3 mm–1.24 mm across. Chemically the hornblende is ferroedenite, near the edenite field, with margins silicic ferroedenite near the silicic edenite field. Chemically the orthopyroxene is ferrohypersthene, which is with Mg content in the range 0.75–0.87 (average Mg=0.80), Fe in the range 1.00–1.12 (average Fe=1.06), Mg/(Mg+Fe)=43%.

Specimen I08² is composed of plagioclase (46%), potash feldspar (22%), quartz (15%), biotite (7%), hornblende (6%), aegirine (2.5%), and riebeckite (0.5%), with accessory amounts of magnetite (1%), apatite (0.1%), and zircon (0.01%). Chlorite, epidote, calcite, and sericite occur as secondary minerals. Hornblende grains 0.5 mm–2.2 mm across occur as euhedral to subhedral prismatic crystals. Grains are ferroedenite, with growths of riebeckite on grain margins (Photo 13). Biotite flakes 0.4 mm–1.7 mm long

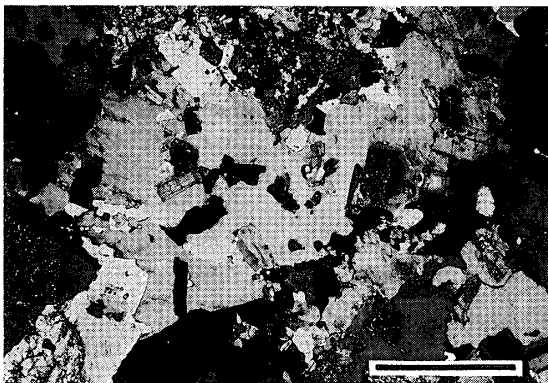


Photo 12. Monzonitic texture: Fine-grained plagioclase and quartz crystals are entrained within coarse-grained potash feldspar. Quartz monzonitic porphyry I07. Nicols crossed. Length of bar: 1mm.

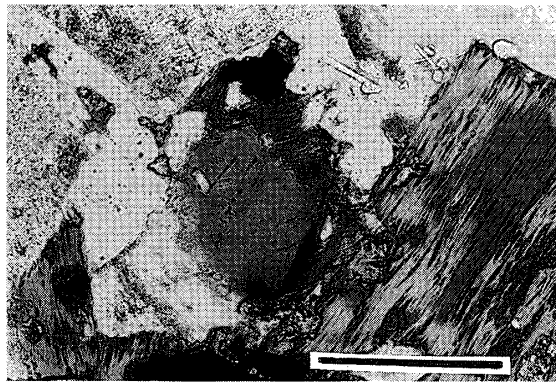


Photo 13. Riebeckite in quartz monzonitic porphyry I08. Riebeckite occupies marginal deep-coloured part around central hornblende. One nicol. Length of bar: 0.2mm.

Table 8. Chemical compositions of aegirine and aegirine-augite in quartz monzonitic porphyry (I08²), and of aegirine in the Kuiqi granite (Suwa et al., 1987)

	Aegirine		Aegirine-augite		Aegirine-augite		Aegirine (Kuiqi Gr)	
SiO ₂	53.22		53.58		52.04		52.3	
TiO ₂	4.33		6.54		0.16		0.05	
Al ₂ O ₃	0.16		0.11		0.39		0.25	
Cr ₂ O ₃	0.00		0.00		0.00		0.00	
Fe ₂ O ₃	24.99		20.71		10.11		} 32.9	
FeO	2.56		0.74		9.16			
MnO	0.10		0.24		0.50		0.15	
MgO	1.03		3.54		5.96		0.25	
NiO	0.00		0.06		0.00		0.00	
CaO	0.69		2.07		16.49		1.17	
Na ₂ O	13.15		12.93		4.26		12.9	
K ₂ O	0.00		0.00		0.03		0.01	
Total	100.23		100.52		99.10		99.98	
Si	2.012	2.012	1.991	} 1.996	2.012	2.012	2.005	2.005
Al	0.007	} 0.983	0.005		} 0.990	0.018	} 0.973	0.011
Ti	0.123		0.183	0.005		0.005		
Cr	0.000		0.000	0.000		0.000		
Fe ³⁺	0.711		0.579	0.294		0.294		
Fe ²⁺	0.081		0.023	0.296		0.296		
Mn	0.003	0.007	0.017	0.017				
Mg	0.058	0.196	0.343	0.343				
Ni	0.000	0.002	0.000	0.000				
Ca	0.028	0.082	0.683	0.683				
Na	0.964	} 0.992	0.932	} 1.014	0.319	} 1.003	0.959	} 1.008
K	0.000		0.000		0.001		0.001	

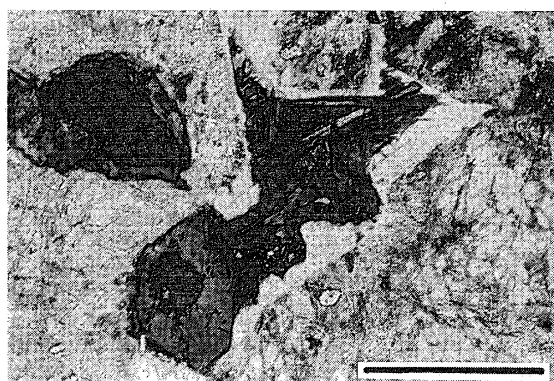


Photo 14. Aegirine-augite in quartz monzonitic porphyry I08. Aegirine-augite occupies grain boundaries between earlier crystallized grains. One nicol. Length of bar: 0.5mm.

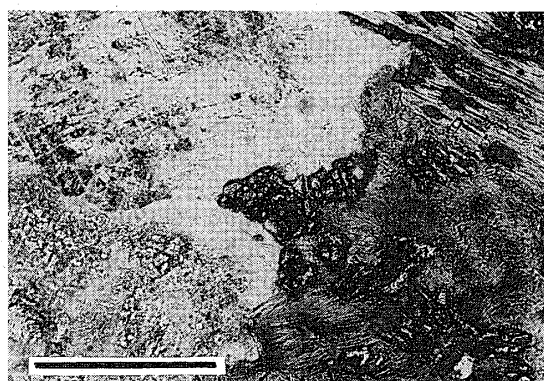


Photo 15. Aegirine in quartz monzonitic porphyry I08. Aegirine occupies central part of Photo 15. One nicol. Length of bar: 0.2mm.

are dark brown and strongly pleochroic. Plagioclase occurs as euhedral to subhedral prismatic platy crystals 0.74 mm–2.3 mm across and is assumed to have crystallized simultaneously and/or just after hornblende and biotite. Normal and oscillatory zoning is common. Plagioclase has a composition in the range Ab77.1–Ab51.4, An45.8–An22.2, Or2.9–Or0.7.

Outer-most rims are almost pure albite with Ab99.1, An0.0, Or0.9. Potash feldspar occurs as anhedral grains 0.3 mm–2.4 mm across, with a composition of Or74.1–Or68.5 (average Or71.4), Ab30.8–Ab25.4 (average Ab28.1), An0.7–An0.3 (average An0.5). The outermost rims have the composition Or91.3, Ab8.7, An0.0. Quartz occurs as irregular anhedral crystals 0.16 mm–1.5 mm across with undulatory extinction, and formed along the grain boundaries of other minerals. According to EPMA analyses, aegirine-augite occurs as radial aggregates, and aegirine occurs as fine-grained individual crystals. Chemical compositions of alkali pyroxenes are shown in Table 8.

In Table 8, chemical composition of the aegirine in the Kuiqi granite is also shown for reference. The Kuiqi granite occurs around Fuzhou (26.1° N, 119.3° E), southeastern China. The Rb-Sr isochron age of the Kuiqi granite is 108Ma. The Kuiqi granite body is characterized by an enrichment in miarolitic cavities, which are filled mainly by orthoclase, anorthoclase, albite, quartz, Zn-Mn ilmenite, fluorite, aegirine and arfvedsonite, with accessory zircon, magnetite, hematite and sphalerite (Suwa et al., 1987).

In the quartz monzonitic porphyry (I08²), alkali amphibole (riebeckite) and alkali pyroxene (aegirine, aegirine-augite) occur along the margins of hornblende and biotite grains (Photos 13, 14 and 15). Similar occurrence of alkali amphibole is clearly observed in the grey granite in the Seychelles (Hoshino, 1986 and Suwa et al., 1994). The grey granite is an alkaline A-type granite and its apparent Rb-Sr isochron age is 570±5Ma. The grey granite consists of microcline-mesoperthite, quartz, ferrichterite-ferrowinchite, ferroactinolite, riebeckite, ferrohedenbergite and annite with accessories of albite, fluorite, sphene, apatite, zircon, allanite, magnetite and ilmenite.

Acknowledgements

We express our sincere thanks to Professor Wang Dezi of Nanjing University for his most esteemed and invaluable guidance. We are very grateful to Professors Kazuhiro Suzuki and Masaki Enami of Nagoya University for their kind assistance with EPMA analysis.

REFERENCES

- Hoshino, M. (1986). Amphiboles and coexisting ferromagnesian silicates in granitic rocks in Mahe, Seychelles. *Lithos*, **19**, pp. 11–25.
- Suwa, K., Enami, M., Hiraiwa, I., and Tai-ming Yang (1987). Zn-Mn ilmenite in the Kuiqi granite from Fuzhou, Fujian province, east China. *Mineralogy and Petrology*, **36**, pp. 111–120.
- Suwa, K., Tokieda, K., and Hoshino, M. (1994). Palaeomagnetic and petrological reconstruction of the Seychelles. *Precambrian Research*, **69**, pp. 281–292.
- Wang Dezi and Zhou Jincheng (1986). An autoclastic volcanic-intrusive rock and its metallogenic relations. In: *Advances in Science of China: Earth Sciences*, Vol. 1, Edited by Tu Guangzhi, Science Press, Beijing, China, 1986, John Wiley and Sons, New York, pp. 133–150.